Articles

Oxygen and Hydrogen Isotope Effects in an Active Site Tyrosine to Phenylalanine Mutant of Peptidylglycine α-Hydroxylating Monooxygenase: Mechanistic Implications†

Wilson A. Francisco,‡,§ Ninian J. Blackburn,|| and Judith P. Klinman*,‡

Departments of Chemistry and Molecular and Cell Biology, University of California, Berkeley, California 94720-1460, and Department of Biochemistry and Molecular Biology, OGI School of Science and Engineering at OHSU, 20000 NW Walker Road, Beaverton, Oregon 97006-8921

Received September 20, 2002; Revised Manuscript Received November 26, 2002

ABSTRACT: Peptidylglycine α-hydroxylating monooxygenase (PHM) and dopamine β-monooxygenase (Dβ M) are homologous copper-containing enzymes that catalyze an oxygen-dependent hydroxylation of peptide-extended glycine residues and phenethylamines, respectively. The mechanism whereby these enzymes activate molecular oxygen and the C−H bond of substrate has been the subject of numerous studies, and various mechanisms have been put forth. From the magnitude of ^{18}O isotope effects as a function of substrate structure in Dβ M, an active site tyrosine had been proposed to function in the reductive activation of Cu(II)−OOH to generate a reactive copper−oxo species [Tian et al. (1994) *Biochemistry 33*, 226]. The presence of a tyrosine residue, Y318, in the active site of PHM was subsequently confirmed from crystallographic studies [Prigge et al. (1997) *Science 278*, 1300]. We now report extensive kinetic and isotope effect studies on the Y318F mutant form of PHM, analyzing the role of this tyrosine in the catalytic mechanism. It is found that the Y318F mutant has intrinsic hydrogen and ^{18}O isotope effects that are within experimental error of the wild-type enzyme and that the mutation causes only a slight reduction in the rate constant for C−H bond cleavage. These findings, together with the recent demonstration that C−H activation in PHM is dominated by quantum mechanical tunneling [Francisco et al. (2002) *J. Am. Chem. Soc. 124*, 8194], necessitate a reexamination of plausible mechanisms for this unique class of copper enzymes.

A posttranslational, C-terminal amidation of peptides is commonly required for the generation of a large class of bioactive, signaling molecules. This modification is carried out by the bifunctional enzyme peptidylglycine α-amidating monooxygenase (PAM;[1] EC 1.14.17.3). The first enzyme activity, peptidylglycine α-hydroxylating monooxygenase (PHM), derives from a copper-containing protein that catalyzes an oxygen- and ascorbate-dependent stereospecific hydroxylation at the α carbon of the C-terminal glycine (Scheme 1). This hydroxylated intermediate is converted to the final product by the action of the second enzyme activity, peptidyl-α-hydroxyglycine α-amidating lyase (PAL; EC 4.3.2.15). For recent reviews on C-terminal peptide amidation and the structure, mechanism, and function of PHM, see refs *1* and *2*.

Scheme 1: Overall Reaction Catalyzed by the Peptidylglycine α-Amidating Monooxygenase[a]

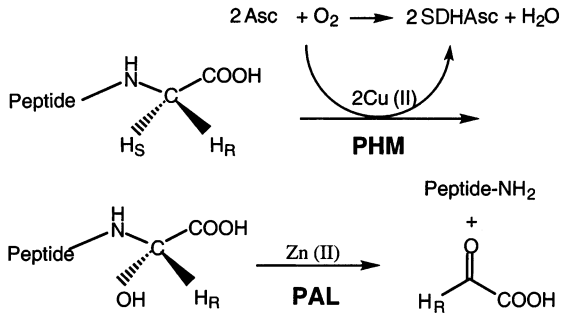

[a] In this scheme the α-hydroxylating monooxygenase (PHM) is analogous to dopamine β-monooxygenase (Dβ M). The hydroxylated intermediate is cleaved by peptidyl-α-hydroxyglycine α-amidating lyase (PAL). Asc is ascorbate and SDHAsc is semidehydroascorbate.

Peptidylglycine α-hydroxylating monooxygenase is similar in many respects to the enzyme dopamine β-monooxygenase (Dβ M; EC 1.14.7.1). Their sequences are approximately 30%

† This work was supported by National Institutes of Health Grants GM 25765 to J.P.K. and R01 NS 27583 to N.J.B. W.A.F. was supported by postdoctoral fellowships from the NIH (F32 GM 17026) and the Ford Foundation.

* To whom correspondence should be addressed.

‡ University of California, Berkeley.

§ Current address: Department of Chemistry and Biochemistry, Arizona State University, P.O. Box 871604, Tempe, AZ 85287-1604.

|| OGI School of Science and Engineering at OHSU.

[1] Abbreviations: PAM, peptidylglycine α-amidating monooxygenase; PHM, peptidylglycine α-hydroxylating monooxygenase; PAL, peptidyl-α-hydroxyglycine α-amidating lyase; Dβ M, dopamine β-monooxygenase; PHMcc, catalytic core of PHM; HA, hippuric acid; KIE, kinetic isotope effect; Ac-DiI-YG, *N*-α-acetyl-3,5-diiodotyrosylglycine.

10.1021/bi020592t CCC: $25.00
Published on Web 01/29/2003

Scheme 2: Previously Postulated Mechanism for Dopamine β-Monooxygenase (DβM) in Which an Active Site Tyrosine Reacts with a Copper Hydroperoxide To Generate a Copper−Oxo Species[a]

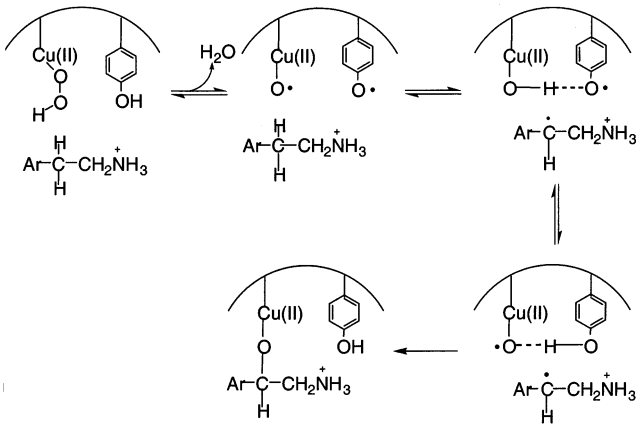

[a] See ref *11*.

identical but exhibit an even greater degree of homology (*3*, *4*). Both enzymes contain two copper atoms and depend on dioxygen and ascorbate for the hydroxylation of an unactivated C−H bond which is believed to proceed via hydrogen atom abstraction (*5*−*9*). The mechanism by which these enzymes activate both oxygen and the C−H bond of substrate has been studied extensively. Various chemical mechanisms have been postulated (*10*−*14*), but a consensus has yet to be reached.

The participation of a tyrosine residue in the catalytic mechanism of DβM has been previously proposed on the basis of mechanism-based inhibition (*15*, *16*) and ^{18}O isotope effect studies (*11*). In the latter case, a mechanism was put forth in which tyrosine is required for the reductive activation of Cu(II)−OOH to generate a copper−oxo species responsible for the hydrogen atom abstraction from substrate (Scheme 2).

The recent crystal structures of the analogous enzyme PHM have confirmed the presence of two tyrosine residues, tyrosines 79 and 318, near the active site (*12*, *13*). These two tyrosine residues are conserved in all PHM and DβM known sequences. In PHM, both tyrosines have been mutated to phenylalanine (Y79F and Y318F), and the mutant enzymes have been preliminarily characterized (*4*, *17*). Initial kinetic analysis of the spent medium from stably transfected CHO cells expressing the mutant enzymes demonstrated that the apparent K_M values of Y79F and Y318F for α-*N*-acetyl-Tyr-Val-Gly were increased approximately 4- and 8-fold, respectively, compared to wild-type PHM. In addition, the Y79F mutant was found to have a slightly reduced V_{max}, and the Y318F mutation was found to have little impact on the apparent V_{max} for the hydroxylation of the tripeptide. However, the known contribution of multiple steps to V_{max} precluded a quantification of the impact of the conserved tyrosines on steps involving substrate and oxygen activation (*18*, *19*).

Tyrosine 318 is found to reside near the CuM site, the site of peptide and oxygen binding, as shown in Figure 1 (*12*, *13*). This residue forms a hydrogen bond with the peptide backbone of the substrate *N*-α-acetyl-3,5-diiodotyrosylglycine in the oxidized (inactive) PHM−substrate crystal structure, providing evidence for a structural but not a

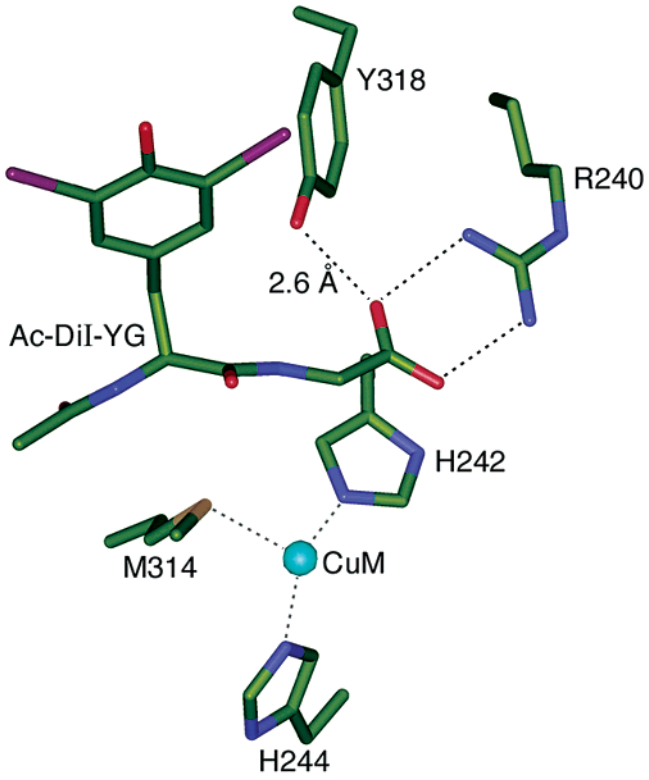

FIGURE 1: Peptide substrate binding to the active site of PHM. Representation of *N*-α-acetyl-3,5-diiodotyrosylglycine (Ac-DiI-YG) bound near the CuM site of PHMcc in the oxidized PHMcc·Ac-DiI-YG crystal structure (*13*). Hydrogen-bonding interactions and Cu−ligand bonds are indicated with dotted lines.

catalytic role for this residue. In the present work, we turned to a detailed analysis of the role of Y318 in the mechanism of PHM by performing extensive kinetic and isotope effect studies on the Y318F mutant form of the enzyme. These studies include initial rate characterizations with labeled peptide and oxygen substrates, allowing us to determine both intrinsic rate constants and isotope effects for Y318F and to compare these parameters with those previously determined for the wild-type enzyme. The results indicate (i) only a 3−4-fold reduction in the rate constant for C−H bond cleavage in Y318F and (ii) intrinsic hydrogen and ^{18}O isotope effects that are within experimental error of the wild-type enzyme.

As a result of the data presented herein, the tyrosine near bound substrate (Y318 in rat PHM and the equivalent Y484 in bovine DβM) can be unambiguously eliminated from playing a role in dioxygen activation. The participation of an active site tyrosine in the reductive cleavage of a Cu(II)−OOH species is concluded to be an unlikely mechanism for this class of enzymes. As we discuss, the previously observed trends in experimental ^{18}O isotope effects as a function of substrate structure (*11*) must be reinterpreted in the context of the present study and the recent demonstration that C−H activation in PHM is dominated by quantum mechanical tunneling (*20*).

MATERIALS AND METHODS

Materials. *N*-Benzoylglycine (hippuric acid), *N*-[benzoyl-2-$^2H_2$]glycine, *N*-[ring-U-^{14}C]benzoylglycine, *N*-[ring-^{3}H]-benzoyl-(2*S*)-[2-$^2H_2$]glycine, and *N*-benzoyl-(*RS*)-[2-^{3}H]-glycine were synthesized as previously described (*18*). [2-$^2H_2$]Glycine was purchased from Cambridge Isotope

Laboratories, Inc. (Andover, MA), catalase was from Boeringer Mannhein Corp. (Indianapolis, IN), and Ecolite (+) liquid scintillation cocktail was from ICN Pharmaceuticals, Inc. (Costa Mesa, CA). All other reagents from commercial sources were of the highest purity available and were used without further purification.

Enzyme Preparation and Purification. The cell lines used to express and purify PHMcc and the mutant Y318F PHMcc were constructed and kindly provided by Drs. Aparna S. Kolhekar, Richard E. Mains, and Betty A. Eipper (Department of Neuroscience, The Johns Hopkins School of Medicine. Mains and Eipper are currently at the Neuroscience Department, University of Connecticut Health Center). Full details of the construction of the cell lines have been reported previously (*17*). PHMcc and Y318F were isolated and purified following a previously described protocol (*14*). The Y318F mutant was further purified by chromatofocusing on a Pharmacia Mono P (HR 5/20) column. The column was equilibrated with 0.025 M bis-Tris-HCl buffer (pH 7.1) and eluted with 10% polybuffer 74 (pH 5.0). The Y318F-containing fractions were collected, pooled, and concentrated in a Centricon concentrator (Amicon). Protein was measured by the bicinchoninic acid (BCA) protein assay (Pierce Chemical Co.) using bovine serum albumin as a standard. The purified sample was >95% pure as judged by SDS−PAGE.

All kinetic and isotope effect experiments described herein were conducted with PHMcc, a truncated version of PHM containing residues 42−356. Kinetic and pH dependence studies of this truncated version of the protein have been reported to yield results similar to those obtained with wild-type PHM and other truncated, but larger, PHM proteins (*17*). Therefore, the notation PHM and PHMcc is used interchangeably in this report.

Noncompetitive Kinetic Isotope Effects. Initial rates were measured from the rate of oxygen consumption at varied oxygen and protiated or dideuterated hippuric acid concentrations. The decrease of oxygen concentration was measured with a YSI model 5300 biological oxygen monitor. The temperature of the chamber was maintained at 37 ± 0.1 °C with a Neslab circulating water bath. Reaction mixtures (1 mL) contained 100 mM MES (pH 6.0), 30 mM KCl, 10 mM sodium ascorbate, 10 μg/mL catalase, 1 μM $CuSO_4$, and various amounts of hippuric acid substrate (2.5−20 mM) at a range of concentrations of dissolved oxygen (60−970 μM). Individual reaction mixtures were made from stock solutions with addition of concentrated solutions of ascorbate, catalase, and $CuSO_4$. The oxygen concentration was varied by stirring the reaction mixtures for at least 15 min with premixed O_2/N_2 mixtures in the appropriate proportions to yield the desired O_2 concentration. The resulting oxygen concentration was determined from the known concentration of dissolved oxygen in air-saturated water (217 μM at 37 °C). Reactions were initiated by the addition of enzyme (2−5 μL). Velocities of both unlabeled and dideuterated substrates at a given concentration were obtained in a single experiment using the same stocks of the other reaction components to minimize fluctuations in experimental conditions. Data obtained by varying the concentration levels of the two substrates were fitted to eqs 1 and 2 describing an equilibrium-ordered mechanism and a two-substrate steady-state mechanism, respectively, using the programs of Cleland (*21*):

$$v = \frac{VAB}{K_{ia}K_b + K_bA + AB} \quad (1)$$

$$v = \frac{VAB}{K_{ia}K_b + K_bA + K_aB + AB} \quad (2)$$

where A and B are the substrate concentrations, V is the maximal velocity, K_a and K_b are the Michaelis constants for A and B, respectively, and K_{ia} is the dissociation constant of A.

Competitive Kinetic Isotope Effects and Intrinsic Isotope Effects. The measurement of the competitive primary deuterium [$^D(V/K)_{HA}$], primary tritium [$^T(V/K)_{HA}$], and secondary tritium [$^{\alpha-T}(V/K)_{HA}$] isotope effects on V/K for hippuric acid was performed in 100 mM MES (pH 6.0), 30 mM KCl, 10 mM sodium ascorbate, 15 mM potassium iodide, and 100 μg/mL catalase under an atmosphere of oxygen, as described previously (*18*). Primary and α-secondary deuterium intrinsic isotope effects were calculated using Northrop's method (*22*) from deuterium and tritium isotope effects on V/K measured in a competitive fashion as described (*18*); this calculation assumes that primary and α-secondary hydrogen isotope effects arise from the same step.

Oxygen Kinetic Isotope Effects. The experimental apparatus designed for oxygen isotope effect experiments (*11*, *23*) was used with slight modifications. The ^{18}O isotope effects were measured at 20 °C in 100 mM MES (pH 5.5 or 6.0), 30 mM KCl, 10 mM sodium ascorbate, 100 μg/mL catalase, 1% ethanol, and 10 mM hippuric acid (protiated or dideuterated). The final reaction volume was approximately 40 mL, which allowed for the collection of two samples of approximately 15 mL each per experiment. The first sample was used to determine the quantity and isotopic composition of dioxygen at the beginning of the experiment. To start the enzymatic reaction, various amounts of enzyme (PHMcc or Y318F) were injected into the vessel through a septum immediately after the first time point was collected. The second sample was collected after a given time period to determine the quantity and isotopic composition of dioxygen corresponding to various extents of conversion. Isolation of unreacted dioxygen, conversion to CO_2, and isotopic analysis have been described elsewhere (*11*, *23*). The data were fitted to eq 3 by nonlinear regression using the program Mathematica:

$$R/R_0 = (1 - f)^{[1/(^{18}(V/K))]-1} \quad (3)$$

where R and R_0 are the isotope ratios ($^{18}O/^{16}O$) in the sample and the blank, respectively, and f is the extent of reaction.

RESULTS AND DISCUSSION

Kinetic Mechanism for Y318F PHM. Initial velocity measurements were performed with Y318F as a function of hippuric acid (protiated and deuterated) and oxygen. The double-reciprocal plots of the initial rate versus 1/[HA] and 1/[O_2] intersect on the left of the 1/v axis above the horizontal axis, characteristic of steady-state-ordered or -random mechanisms (data not shown). However, since the kinetic order for HA with WT-PHM is equilibrium ordered (*18*), the initial velocity data were fitted to eqs 1 and 2 (Materials and Methods) describing an equilibrium-ordered and a steady-

Table 1: Kinetic Parameters for Y318F and Wild-Type PHM with Hippuric Acid (HA) as Substrate

	Y318F[a]			wild-type PHM[b]		
parameter	$[^1H_2]$HA	$[^2H_2]$HA	IE[c]	$[^1H_2]$HA	$[^2H_2]$HA	IE[c]
k_{cat} (s^{-1})[d]	27.6 ± 1.2	13.6 ± 2.9	2.03 ± 0.44	39.1 ± 0.5	25.0 ± 1.1	1.56 ± 0.07
k_{cat}/K_m (HA) (mM^{-1} s^{-1})[d]	15.9 ± 2.9	1.91 ± 0.40	8.32 ± 2.32	NA[e]	NA[e]	NA[e]
k_{cat}/K_m (O_2) (mM^{-1} s^{-1})	99.2 ± 5.8	12.3 ± 1.2	8.10 ± 0.91	185.0 ± 0.6	58.3 ± 3.9	3.17 ± 0.21
K_i (HA) (mM)	22.0 ± 1.4	7.0 ± 1.1	3.15 ± 0.54	2.9 ± 0.1	4.5 ± 0.4	0.64 ± 0.06

[a] Kinetic parameters obtained by fitting the initial velocity data to the equation describing a sequential mechanism (eq 2) using the programs of Cleland (*21*). Experimental conditions: 100 mM MES, pH 6.0, 30 mM KCl, 10 μg/mL catalase, 1 μM $CuSO_4$, 10 mM ascorbic acid, and varying amounts of protiated and dideuterated hippuric acid and oxygen at 37 °C. [b] Taken from Francisco et al. (*18*). [c] IE, isotope effect. [d] K_m (O_2) for $[^2H_2]$hippuric acid is ca. 1 mM, the highest concentration achievable. Hence, both k_{cat} and k_{cat}/K_M at infinite O_2 can only be achieved by extrapolation, leading to larger errors than with protiated substrate. [e] NA, not applicable.

Scheme 3: Random Kinetic Mechanism for the Y318F Variant of Peptidylglycine α-Hydroxylating Monooxygenase (PHM)

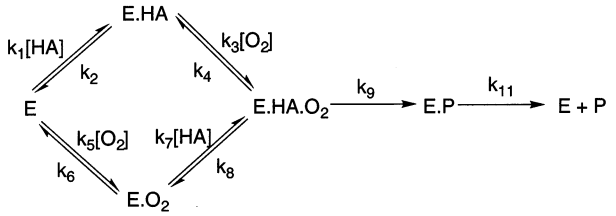

Table 2: Competitive Hydrogen Isotope Effects for Y318F and Wild-Type PHM

parameter	Y318F[a]	wild-type PHM[b]
$^D(V/K)_{HA}$	4.51 ± 0.07	3.88 ± 0.05
$^T(V/K)_{HA}$	11.17 ± 0.39	9.73 ± 0.19
$^{\alpha-T}(V/K)_{HA}$	1.11 ± 0.02	1.09 ± 0.01

[a] Experimental conditions: 100 mM MES (pH 6.0), 30 mM KCl, 10 mM sodium ascorbate, 15 mM potassium iodide, and 100 mg/mL catalase under an atmosphere of oxygen at 37 °C. [b] Taken from ref *18*.

state-ordered mechanism, respectively [using the programs of Cleland (*21*)]. A much better fit to the equation describing a steady-state-ordered mechanism (eq 2) was found for the kinetic data of Y318F with both protiated and dideuterated hippuric acid, as determined by the statistical parameter σ, the square root of the residual least squares (*21*). The σ values for the fit to eqs 1 and 2 are 0.71 and 0.03, respectively, for the protiated hippuric acid data and 0.53 and 0.09, respectively, for the dideuterated hippuric acid data. The kinetic parameters obtained from the fit to eq 1 of the Y318F data are summarized in Table 1. These data also allowed for the calculation of the isotope effects on k_{cat}, k_{cat}/K_m (HA), k_{cat}/K_m (O_2), and K_i (HA) (Table 1).

Although initial velocity measurements alone do not provide enough information to differentiate between a steady-state-ordered or steady-state-random kinetic mechanism, these can be easily distinguished from the magnitude of the deuterium isotope effect on the kinetic parameter *V*/*K*. It has been demonstrated that the isotope effect on *V*/*K* for the substrate that binds first [$^D(V/K)_A$] is equal to 1 at high concentrations of the second substrate (*24*, *25*). From the data in Table 1, it can be seen that the isotope effects on *V*/*K* for both substrates are large and different from unity at infinite concentration of the alternate substrate. These results eliminate the possibility of a steady-state-ordered mechanism, implicating instead a steady-state-random mechanism for the Y318F mutant of PHM.

The steady-state-random mechanism (Scheme 3) for the Y318F mutant is in contrast to the equilibrium-ordered mechanism for the wild-type enzyme, where the small peptide analogue, hippuric acid, was found to bind first (Scheme 3 with k_5, k_6, k_7, and $k_8 = 0$, $k_2 > k_9$). The substrate-bound structure of wild-type PHM shows that tyrosine 318 forms a hydrogen bond with the C-terminal carboxylate group of the peptide substrate (Figure 1). This 2.6 Å H-bond interaction of Y318 with the peptide substrate, in addition to other protein interactions that include the salt bridge to R240, may be expected to result in an increased association rate constant for peptide substrate and a decrease in the rate constant for substrate release. In the case of extended tri- and tetrapeptides, in which the interactions of the substrate with the active site are likely to be greater than with hippuric acid, peptide binding remains ordered, but with a faster binding rate constant and higher affinity; this latter property results in a steady-state-ordered rather than equilibrium-ordered kinetic mechanism (Francisco et al., in preparation). From the studies herein, it appears that loss of the H-bond between Y318 and the peptide is sufficient to generate indiscriminate substrate binding, such that oxygen competes effectively with hippuric acid for the free form of Y318F.

As mentioned in the introduction, PHM and DβM are similar in numerous respects. The kinetic mechanism of DβM had been found to be dependent on the presence of the activator fumarate. For example, at pH 6.0, the kinetic mechanism of DβM changes from steady-state ordered to steady-state random by elimination of the anion activator fumarate (*5*). The observation of identical kinetic mechanisms with the Y318F PHM mutant and DβM (in the absence of fumarate) extends the similarity between these two enzymes to their kinetic mechanisms.

Intrinsic Hydrogen Isotope Effects for Y318F. The intrinsic isotope effect for an enzymatic reaction can be determined from the measured deuterium and tritium isotope effects on *V*/*K* under identical conditions (*22*). Competitive deuterium, tritium, and α-deuterium isotope effects on $(V/K)_{HA}$ were measured for the Y318F mutant enzyme and are summarized in Table 2 together with previously measured values for the wild-type enzyme. The larger values with Y318F indicate that chemistry is somewhat more rate limiting than for the wild-type enzyme.

The competitively measured $(V/K)_{HA}$ isotope effects were used in the calculation of the primary and α-secondary deuterium intrinsic isotope effects (*18*), which are shown in Table 3. The calculated primary intrinsic isotope effect for the Y318F mutant of 9.4 ± 0.6 is similar to the one calculated for the wild-type enzyme of 10.7 ± 0.4. The

Table 3: Comparison of Intrinsic Hydrogen Isotope Effects for Y318F and Wild-Type PHM with Hippuric Acid as Substrate and DβM with Dopamine as Substrate According to Scheme 3

parameter	Y318F[a]	wild-type PHM[b]	DβM
$^{D}k_9$	9.4 ± 0.6	10.7 ± 0.4	10.9 ± 1.9[c]
$^{\alpha-D}k_9$	1.17 ± 0.02	1.21 ± 0.01	1.19 ± 0.06[d]

[a] Experimental conditions: 100 mM MES (pH 6.0), 30 mM KCl, 10 mM sodium ascorbate, 15 mM potassium iodide, and 100 μg/mL catalase under an atmosphere of oxygen at 37 °C. [b] Taken from ref *18*. [c] Taken from ref *19*. [d] Taken from ref *10*.

calculated α-secondary deuterium intrinsic isotope effects for the Y318F and the wild-type enzyme are 1.17 ± 0.02 and 1.21 ± 0.01, respectively, and are almost within experimental error of one another.

As has been pointed out earlier for wild-type PHM, the primary deuterium intrinsic isotope effect exceeds the semiclassical maximum value of 7, while the α-secondary deuterium intrinsic isotope effect of 1.2 is close to the maximum equilibrium isotope effect expected for the conversion of an sp^3 to sp^2 center. These two observations were taken as suggestive of the contribution of tunneling in the C−H bond cleavage reaction (*18*). The similarity of results with both DβM (*10*, *19*) and now Y318F PHM (Table 3) implicates consistently analogous behavior. This tunneling hypothesis has been further pursued by investigation of the temperature dependence of the intrinsic isotope effect in wild-type PHM. The finding that the intrinsic isotope effects are nearly temperature independent now provides direct evidence for nonclassical behavior in the reaction catalyzed by PHM (*20*). The magnitudes of the parameters describing the hydrogen-transfer step in wild-type PHM have been interpreted in the context of an environmentally coupled hydrogen tunneling model that is described by a ligand reorganization term and a gating frequency for the heavy atoms that modulate the hydrogen tunneling event (*20*). The small reduction in the magnitude of the intrinsic primary isotope effect for the Y318F mutant of PHM may indicate a greater role for gating than with the wild-type enzyme. It would appear that the more open and less organized an active site, the greater the role for gating in achieving the internuclear distances required for tunneling (*20*).

Impact of Y318F on Binding and Chemical Steps. Intrinsic rate constants for the minimum kinetic mechanism shown in Scheme 3 can be calculated from the measured kinetic parameters, their isotope effects, and the intrinsic isotope effects. This methodology has been previously used for the calculation of the rate constants of the reactions catalyzed by DβM (*5*) and wild-type PHM (*18*). The microscopic rate constants calculated for the Y318F mutant are shown in Table 4. It can be seen that the Y318F mutation affects the rate of most steps, but most notably k_4 and k_9. An approximately 3-fold increase is seen in the dissociation constant for O_2 from the ternary complex and an approximately 3-fold decrease is seen in the rate of the C−H bond cleavage step. As described above, the kinetic mechanism for this mutant is steady-state random compared to the rapid-equilibrium-ordered mechanisms reported for the wild-type enzyme. As a result, two more rate constants, k_7 and k_8 in Scheme 3, corresponding to the association and dissociation of hippuric acid from the E·O_2 binary complex, can be calculated. The error in these rate constants, however, is comparable to the rate constants themselves, in large part due to the errors in $^{D}(k_{cat}/K_m)_{HA}$ and $^{D}k_{cat}$ that result from a large K_m (O_2) for [$^2H_2$]hippuric acid of approximately 1 mM (the highest concentration of dissolved oxygen attainable at 37 °C and atmospheric pressure).

Table 4: Intrinsic Rate Constants for Y318F and Wild-Type PHM According to Scheme 3

constant	Y318F[a]	wild-type PHM[b]
k_3 (mM^{-1} s^{-1})	330 ± 130	227 ± 7
k_4 (s^{-1})	635 ± 320	185 ± 28
k_7 (mM^{-1} s^{-1})	(59 ± 59)[c]	NA[d]
k_8 (s^{-1})	(720 ± 870)[c]	NA[d]
k_9 (s^{-1})	268 ± 114	810 ± 120
k_{11} (s^{-1})	31 ± 2	41 ± 1

[a] Calculated from the equations derived in ref *5* (eqs 1−8, Table 6) using the product of the intrinsic primary and α-secondary isotope effect, 11.0 ± 0.7 for Y318F and 12.7 ± 1.0 for wild-type PHM, as discussed in ref *18*. [b] Taken from ref *18*. [c] These parameters are underdetermined due to the large propagated errors. [d] NA, not applicable.

Table 5: $^{18}(V/K)$ Isotope Effects for Wild-Type and Y318F PHM and DβM

substrate	PHM[a]	Y318F[a]	DβM[b]
protiated	1.0173 ± 0.0009	1.0169 ± 0.0014	1.0197 ± 0.0003
deuterated	1.0212 ± 0.0018	ND[c]	1.0256 ± 0.0003

[a] Data were collected at pH 5.5 or 6.0, 25 °C, in 100 mM MES, 30 mM KCl, 10 mM sodium ascorbate, 100 μg/mL catalase, and 1% ethanol with 10 mM hippuric acid or [$^2H_2$]hippuric acid as substrates. [b] Data from ref *11* collected at pH 5.5, 25 °C, and 10 mM fumarate using 3-hydroxytyramine and [2,2-$^2H_2$]-3-hydroxytyramine as substrates. [c] ND, not detemined.

Oxygen-18 Kinetic Isotope Effects (^{18}O KIEs). Oxygen-18 kinetic isotope effects, as a function of deuteration of the substrate dopamine, have been reported for the reaction catalyzed by DβM (*11*). These isotope effects were measured competitively with a technique that allows the precise determination of ^{18}O KIEs using natural abundance ^{18}O. In this study, the same technique was used to measure ^{18}O KIEs in the reaction catalyzed by PHM with protiated and dideuterated hippuric acid, indicating values for $^{18}(V/K)$ of 1.0173 ± 0.0009 and 1.0212 ± 0.0018, respectively (Table 5). These experimental isotope effects are similar to those measured previously for DβM using protiated and deuterated dopamine (Table 5) (*11*). Tian et al. have presented a method for the calculation of the intrinsic ^{18}O isotope effect (^{18}k) from the measured deuterium and ^{18}O kinetic isotope effects on V/K, as shown below (*11*), where the increase in $^{18}(V/K)$ with deuteration is ascribed to an overall increased rate limitation by chemistry:

$$^{18}k = \frac{^{D}(V/K)\,^{18}(V/K)_D - {}^{18}(V/K)_H}{^{D}(V/K) - 1} \quad (4)$$

This equation assumes that the C−H bond cleavage is irreversible, which has been demonstrated for DβM (*19*). Note that ^{18}k reflects all changes in bond order at O_2 up through the irreversible C−H cleavage step. A value for ^{18}k of 1.0230 ± 0.012 can be calculated for PHM with hippuric acid. Despite the large propagated error, this is seen to be identical to the value of 1.0281 ± 0.0012, previously calculated for DβM with dopamine as substrate (*11*). It appears that PHM and DβM, working with different sub-

strates, have conserved the size of both the intrinsic deuterium (*18*; Table 3) and ^{18}O kinetic isotope effects (*11*; Table 5).

The PHM reaction is the second example of a measured ^{18}O isotope effect that is dependent on substrate deuteration. The significance of this observation deserves further consideration. Given that $^{18}(V/K)$ reflects all steps from oxygen binding through the first irreversible step, the sensitivity of the oxygen isotope effect to substrate deuteration means that *C−H cleavage must be connected to the activation of* O_2 *through a series of fully reversible steps*. This has important implications for the nature of the activated oxygen species that precedes C−H cleavage and will be discussed in greater detail below.

According to the mechanism put forth in Tian et al. for the DβM reaction (*11*), a tyrosine residue in the active site plays an essential role in the mechanism of oxygen activation (where Y484 in bovine DβM corresponds to Y318 in PHM). Although the mutagenesis experiments described above indicate that Tyr 318 is not essential for chemistry in PHM, it appeared possible that an alternate pathway with a different mechanism for oxygen activation could come into play in the absence of Y318. We therefore measured the oxygen isotope effect with Y318F. As shown in Table 5, an $^{18}(V/K)$ of 1.0169 ± 0.0014 is observed for protiated hippuric acid with Y318F. This value is essentially identical to the 1.0173 ± 0.0009 obtained with protiated hippuric acid and the wild-type enzyme. Due to the large amounts of enzyme needed for these measurements, it was not possible to determine the ^{18}O KIE for the slower reaction of dideuterated hippuric acid with Y318F, precluding an estimate of the intrinsic ^{18}O isotope effect for the mutant enzyme. Nonetheless, the identity of the measured isotope effects with both wild-type and mutant enzymes indicates a similar mechanism for dioxygen activation.

Implications for the Chemical Mechanism of DβM and PHM. The compelling sequence and chemical homology between PHM and DβM support a highly conserved active site structure and reaction mechanism within this enzyme class. One of the major observations that led to the proposal of reductive cleavage of hydrogen peroxide by an active site residue (tyrosine) in DβM was the observed decrease in measured ^{18}O kinetic isotope effects as a function of decreasing substrate phenethylamine reactivity. As discussed in the paper by Tian et al. (*11*), the magnitude of the ^{18}O isotope effects was, in fact, expected to increase as the reactivity of substrate decreased if the activating oxygen species were Cu(II)−OOH. The reason for this expectation was the Hammond postulate, which posits a correlation between reaction driving force and the degree to which transition state structure for hydrogen transfer is early or late. The observation of a high degree of quantum mechanical tunneling in the PHM reaction indicates, however, that this is no longer an appropriate context in which to interpret trends in the ^{18}O isotope effects. In the case of the environmentally modulated tunneling model that has been used to model the behavior of PHM (*20*), the barrier to reaction is the heavy atom motions that control tunneling. There are three major factors that will impact the nature of this heavy atom barrier; these are the reaction driving force ($\Delta G°$), heavy atom ligand reorganizations (λ), and the gating frequency for heavy atom modulation of the distance between reactants (ωx) (cf. ref *26*). The heavy atom isotope effects are, thus, expected to reflect any preequilibrium chemical steps that occur at the molecular oxygen, together with changes in the heavy atom barriers that control tunneling. Work is currently in progress to understand the origin of ^{18}O isotope effects in outer-sphere electron-transfer processes (Klinman and Roth, in preparation) and is expected to impact the interpretation of the magnitude and trends of ^{18}O kinetic isotope effects in the hydrogen transfer catalyzed by PHM and DβM.

Thus, there are now three critical pieces of data that "frame" our understanding of oxygen reactivity in PHM and DβM. These are (i) that the transfer of hydrogen from substrate to activated oxygen occurs by a tunneling process, obviating the use of classical physical organic probes to interpret trends in ^{18}O isotope effects, (ii) the finding that replacement of the active site tyrosine by phenylalanine has only a modest effect on the rate of the chemical step of catalysis and practically no effect on the deuterium and oxygen isotope effects, and (iii) that the deuterium substitution on substrate increases the measured ^{18}O isotope effect for *both* PHM and DβM. These data call into question a mechanism in which a Cu(II)−OOH is reductively cleaved by an active site tyrosine (Scheme 2). In direct opposition to the current observations, the mechanism in Scheme 2 predicts a significant effect of the conversion of Y318 to a phenylalanine on both rate and isotope effects. Additionally, reductive cleavage of a copper−hydroperoxy intermediate to a copper−oxo species, involving oxidation of two copper centers that lie ca. 10 Å apart (Figure 1) and the loss of a water molecule, is expected to be irreversible. The resulting uncoupling of dioxygen activation from C−H activation would produce an ^{18}O isotope effect that is independent of substrate deuteration, in contrast to the experimental observations.

Where do these observations lead us with regard to the nature of the activated oxygen species in the DβM and PHM reactions? As noted by Priegge et al. (*12*, *13*), there is no general acid in the active site of PHM, and a copper−hydroperoxy anion, rather than copper hydroperoxide, was proposed as the oxidizing species (*2*). One question that needs to be addressed, however, is whether a long-range electron transfer (ca. 10 Å) from the CuH side to a CuM−dioxygen complex could occur in a reversible process and/or be mediated by the movement of a one-electron form of O_2 ($O_2^{\bullet-}$) across the large cleft (*14*). If this is not the case, then yet a different species must be responsible for C−H activation in PHM and DβM. Work is currently in progress in this laboratory to address this challenging question.

ACKNOWLEDGMENT

We thank Drs. Betty E. Eipper and Richard E. Mains for kindly providing the cell lines used for the expression of PHMcc and the Y318F mutant. We are also grateful to Frank Rhammes for the purification of the PHMcc and to Shulamit Jaron for the purification of the Y318F mutant.

REFERENCES

1. Kulathila, R., Merkler, K. A., and Merkler, D. J. (1999) *Nat. Prod. Rep. 16*, 145−154.
2. Prigge, S. T., Mains, R. E., Eipper, B. A., and Amzel, L. M. (2000) *Cell. Mol. Life Sci. 57*, 1236−1259.

3. Southan, C., and Kruse, L. I. (1989) *FEBS Lett. 255*, 116−120.
4. Eipper, B. A., Quon, A. S. W., Mains, R. E., Boswell, J. S., and Blackburn, N. J. (1995) *Biochemistry 34*, 2857−2865.
5. Ahn, N., and Klinman, J. P. (1983) *Biochemistry 22*, 3096−3106.
6. Fitzpatrick, P. F., and Villafranca, J. J. (1987) *Arch. Biochem. Biophys. 257*, 231−250.
7. Bradbury, A. F., Mistry, J., Roos, B. A., and Smyth, D. G. (1990) *Eur. J. Biochem. 189*, 363−368.
8. Katopodis, A. G., and May, S. W. (1990) *Biochemistry 29*, 4541−4548.
9. Zabriskie, T. M., Cheng, H. M., and Vederas, J. C. (1992) *J. Am. Chem. Soc. 114*, 2270−2272.
10. Miller, S. M., and Klinman, J. P. (1985) *Biochemistry 24*, 2114−2127.
11. Tian, G. C., Berry, J. A., and Klinman, J. P. (1994) *Biochemistry 33*, 226−234.
12. Prigge, S. T., Kolhekar, A. S., Eipper, B. A., Mains, R. E., and Amzel, L. M. (1997) *Science 278*, 1300−1305.
13. Prigge, S. T., Kolhekar, A. S., Eipper, B. A., Mains, R. E., and Amzel, L. M. (1999) *Nat. Struct. Biol. 6*, 976−983.
14. Jaron, S., and Blackburn, N. J. (1999) *J. Inorg. Biochem. 74*, 180−180.
15. Dewolf, W. E., Carr, S. A., Varrichio, A., Goodhart, P. J., Mentzer, M. A., Roberts, G. D., Southan, C., Dolle, R. E., and Kruse, L. I. (1988) *Biochemistry 27*, 9093−9101.
16. Farrington, G. K., Kumar, A., and Villafranca, J. J. (1990) *J. Biol. Chem. 265*, 1036−1040.
17. Kolhekar, A. S., Keutmann, H. T., Mains, R. E., Quon, A. S. W., and Eipper, B. A. (1997) *Biochemistry 36*, 10901−10909.
18. Francisco, W. A., Merkler, D. J., Blackburn, N. J., and Klinman, J. P. (1998) *Biochemistry 37*, 8244−8252.
19. Miller, S. M., and Klinman, J. P. (1983) *Biochemistry 22*, 3091−3096.
20. Francisco, W. A., Knapp, M. J., Blackburn, N. J., and Klinman, J. P. (2002) *J. Am. Chem. Soc. 124*, 8194−8195.
21. Cleland, W. W. (1979) *Methods Enzymol. 63*, 103−138.
22. Northrop, D. B. (1975) *Biochemistry 14*, 2644−2651.
23. Tian, G. C., and Klinman, J. P. (1993) *J. Am. Chem. Soc. 115*, 8891−8897.
24. Klinman, J. P., Humphries, H., and Voet, J. G. (1980) *J. Biol. Chem. 255*, 1648−1651.
25. Cook, P. F., and Cleland, W. W. (1981) *Biochemistry 20*, 1790−1796.
26. Knapp, M. J., Rickert, K., and Klinman, J. P. (2002) *J. Am. Chem. Soc. 124*, 3865−3874.
27. Mendenhall, W. (1983) *Introduction to Probability and Statistics*, 6th ed., Duxbury, Boston, MA.

BI020592T